Journal of Organometallic Chemistry, 435 (1992) 319–335
Elsevier Sequoia S.A., Lausanne
JOM 22663

Structural properties of cationic molybdenum and tungsten allyl derivatives

Brian J. Brisdon, Michael Cartwright, Annabelle G.W. Hodson, Mary F. Mahon and Kieran C. Molloy

School of Chemistry, University of Bath, Claverton Down, Bath BA2 7AY (UK)

(Received December 31, 1991)

Abstract

Cationic allyldicarbonyl derivatives of molybdenum and tungsten of the types $[M(CO)_2(\eta^3\text{-allyl})(L_3)]PF_6$ (M = W, allyl = C_3H_5 or 2-MeC_3H_4, L_3 = bis(2-pyridylmethyl)amine, bpma) and $[M(CO)_2(\eta^3\text{-allyl})(L_4)]PF_6$ (M = Mo or W, allyl = C_3H_5 or 2-MeC_3H_4, L_4 = tris(2-pyridylmethyl)amine, tpma) have been prepared, and their isomerism and dynamic behaviour in solution examined. In the solid state, $[W(CO)_2(\eta^3\text{-}C_3H_5)(bpma)]PF_6$ (**1a**) exhibits an unsymmetric, and $[Mo(CO)_2(\eta^3\text{-}C_3H_5)(tpma)]PF_6$ (**3**) a symmetric, orientation of the N-donor set, which comprises two pyridyl rings and the central, exocyclic N of each ligand, with respect to the π-allyl group. The third bipyridyl ring of tpma in the latter complex is orientated away from the metal centre in the solid, but undergoes rapid exchange with N-donors within the coordination sphere at elevated temperatures in solution. Neither of the 2-MeC_3H_4 analogues of **3** are dynamic under similar conditions, whereas the 2-MeC_3H_4 analogue of **1** undergoes a facile trigonal twist rearrangement.

Introduction

In an earlier paper [1], we described the preparation and characterisation of cationic molybdenum(II) species of the type $[Mo(CO)_2(\eta^3\text{-allyl})(L_3)]^+$ (L_3 = diethylenetriamine or bis(2-pyridylmethyl)amine). NMR spectroscopy was used to show that the cations were dynamic in solution at ambient temperature, and that a restricted trigonal twist rearrangement involving enantiomeric interconversions as illustrated by Ia and Ib, accounted fully for the spectral observations.

Recently Shiu *et al.* [2,3] have shown that chromium, molybdenum and tungsten analogues containing the neutral tridentates *N,N*-bis(pyrazol-1-ylmethyl)aminomethane (bpam) or *N,N*-bis[(3,5-dimethylpyrazol-1-yl)methyl]aminomethane

Correspondence to: Dr. B.J. Brisdon, School of Chemistry, University of Bath, Bath BA2 7AY, UK.

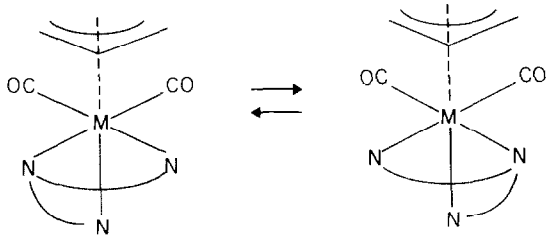

Ia Ib

(bdmpam) adopt either an unsymmetrical structure (I) or a symmetrical structure (II), depending upon a fine balance between electronic and steric effects.

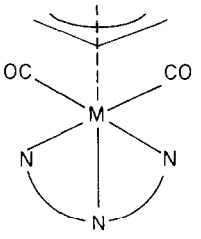

II

They also claimed that these two compounds provided the first dynamic examples among all the η^3-allyl dicarbonyl complexes containing a neutral chelate, and they proposed an unusual five-stage rearrangement process to account for the stereochemical non-rigidity of $[Mo(bpam)(CO)_2(\eta^3\text{-allyl})]PF_6$. In view of our previous investigations of dynamic and rigid η^3-enyl dicarbonyl complexes of molybdenum which contain neutral nitrogen donor bidentates (L_2) [4], and tridentates (L_3) [1], we were interested in extending our studies to cationic species $[M(CO)_2(\eta^3\text{-}C_3H_4R)(L_4)]^+$ (M = Mo, W; L_4 = potentially quadridentate N-donor ligand). In this paper we report on the synthesis and dynamic properties of four such derivatives, and we also compare their solution behaviour and structural characteristics with those of the cationic tungsten species $[W(CO)_2(\eta^3\text{-}C_3H_4R)(L_3)]^+$ (R = H or 2-Me).

Results and discussion

Complexes **1–6** (Table 1) were readily prepared in high yields by displacement of nitrile and chloride ligands from $MCl(CO)_2(\eta^3\text{-}C_3H_4R)(NCMe)_2$ (M = Mo, W; R = H or Me) on reaction with a stoichiometric quantity of the neutral ligand L_3 or L_4, followed by treatment with aqueous NH_4PF_6. The crude products were recrystallized from aqueous acetone (complexes **1** and **2**) or from aqueous methanol (complexes **3–6**), from which **5** and **6** were isolated as solvates. Complex **1** crystallized as a mixture of two forms, with the major form (labelled **1a** in Table 1) present in large excess (approx. 95% of the total yield). Sufficient of the minor

Table 1

Infrared and microanalytical data

Complex		Yield (%)	ν(CO) [a] (cm^{-1})	ν(XH) [b] (cm^{-1}) (X = N or O)	Anal. Found (calc.)		
					C	H	N
$[W(CO)_2(\eta^3\text{-}C_3H_5)(bpma)]PF_6$	**(1a)**	88 [c]	1948, 1855	3320br	33.1 (32.7)	2.80 (2.88)	6.58 (6.72)
	(1b)		1948, 1855	3320br	33.1 (32.7)	2.88 (2.88)	6.30 (6.72)
$[W(CO)_2(\eta^3\text{-}C_4H_7)(bpma)]PF_6$	**(2)**	79	1940, 1853	3315	33.5 (33.8)	3.02 (3.13)	6.51 (6.57)
$[Mo(CO)_2(\eta^3\text{-}C_3H_5)(tpma)]PF_6$	**(3)**	75	1962, 1870	–	43.5 (42.0)	3.54 (3.66)	8.86 (8.91)
$[W(CO)_2(\eta^3\text{-}C_3H_5)(tpma)]PF_6$	**(4)**	70	1948, 1855	–	38.3 (36.9)	3.16 (3.21)	7.86 (7.82)
$[Mo(CO)_2(\eta^3\text{-}C_4H_7)(tpma)]PF_6 \cdot MeOH$	**(5)**	72	1956, 1866	3410	43.5 (44.5)	4.20 (4.30)	8.33 (8.31)
$[W(CO)_2(\eta^3\text{-}C_4H_7)(tpma)]PF_6 \cdot MeOH$	**(6)**	68	1950, 1857	3650	39.5 (39.4)	3.71 (3.80)	7.59 (7.35)

[a] In CH_2Cl_2. [b] In Nujol. A strong PF_6^- absorption also occurred at 835 ± 5 cm^{-1} in all complexes. [c] Complex **1b** comprised approx. 5% of total yield.

Table 2

^{1}H NMR data [a]

Complex	T (K)	Allyl ligand			Tridentate ligand		
		H_a	H_s	H_c/Me	N–CH_2–C	NH	Aromatics
1a or **1b**	293	1.73d(9.4)	3.33brs	3.36m	4.65d [b] 4.89dd [b]	5.53brs	7.46t, 7.93brs, 8.99m, 9.27brs
1a	193	1.70d(8.9) 1.73d(8.9)	3.20brs 3.59brs	3.38m	4.69d 4.91q [c] 5.13dd [d]	5.89brt	7.45d, 7.50t, 7.66t, 7.73t, 7.97t, 8.08t, 8.99d, 9.37d
2	293	1.79s	3.22s	2.07s	4.59d [b] 4.91dd [b]	5.80brt	7.53t, 7.59t, 8.00dt, 9.04d
	193	1.76s 1.81s	3.12s 3.43s	2.09s	4.47d 4.94q [c] 5.19dd [d]	6.17m	7.43d, 7.59t, 7.66t 7.85d, 8.04t, 8.14t, 9.04d, 9.19d
3	323	1.68brs	3.76brs	3.76brs	4.44brm 4.96brm		7.44brm, 7.86brm, 8.76brm
	211	1.40d(9.6) 1.80d(9.6) 2.03 [e]	3.70brm	3.70brm	4.26d 4.66m 5.20dd 5.94s		7.50m, 7.90m, 8.40d, 8.79d, 8.93d, 9.35d
4	323	1.95brs	3.39brs	3.70brm	4.63brm 5.10brm,		7.33m, 7.43brm, 7.58d, 7.83brm, 8.60d, 8.75brm
	223	1.54d(7.3) [e] 1.93d(7.6) [f] 2.07 [e,g]	3.32m [f] 3.90brm [e]	3.55m [f] 3.90brm [e]	4.48d [e] 4.55d [e] 4.64q [e] 4.70d [f] 5.08d [e] 5.17d [e] 5.30d [f] 5.95s [f]		7.50m, 7.98brm, 8.37d, 8.80d, 8.87d, 8.97d 9.42d
5 [h]	293	1.66s	3.71s	2.16s	4.32d 4.83s 4.98d		7.33d, 7.40t, 7.45m, 7.80brm, 7.92brm, 8.72brs, 8.95brs
6 [h]	293	1.89s	3.52s	2.33s	4.55d 4.87s 5.05d		7.46t, 7.54m, 7.87m, 7.95m, 8.74d, 9.04d

[a] Recorded in $(CD_3)_2CO$ solution. [b] On NH decoupling these signals collapse to a single AB quartet. [c] Weak NH coupling on half of the multiplet. [d] Collapses to a doublet on NH decoupling. [e] Assigned to isomer I. [f] Assigned to isomer II. [g] Partially obscured by solvent absorptions. [h] MeOH signals at 3.31 and 2.99 ppm in each complex.

form (**1b**) was hand picked in order to establish that both forms had very similar analyses, and on dissolution, identical room temperature NMR spectra (Tables 2 and 3), but we were unsuccessful in isolating a crystal of this form suitable for an X-ray structure determination, which would have permitted comparison with the major form for **1a** whose geometry is described below.

Structures of 1a and 3

The asymmetric unit of **1a** contains two molecules of the complex. Bond lengths and angles for these two molecules are only appreciably different within the allyl unit, as can be seen from Table 4. An ORTEP view of the cation of **1a**, and the atomic numbering scheme used, are shown in Fig. 1. This cation adopts the usual

Table 3

$^{13}C\{^1H\}$ NMR data [a]

Complex	CO	Allyl ligand			Tridentate ligand [b]	
		$C_{terminal}$	$C_{central}$	Me	N–CH_2–C	Aromatics
1a	219.8	50.3	62.1		61.6	123.9, 126.3, 140.9, 152.0, 159.0
2	219.4	48.7	74.8	18.4	60.7	123.6, 125.9, 140.3, 151.4, 158.6
3	226.3	57.1	75.7		66.2	123.8, 124.8, 125.9, 127.1, 137.9,
		59.0			66.9	141.1, 150.4, 152.1, 152.9, 153.4,
					69.4	157.6, 159.0
					71.6	
4	219.5	49.5	63.9		66.0	123.9, 124.8, 126.6, 127.3, 138.0,
		51.1			67.3	140.2, 141.6, 149.7, 150.5, 152.5,
		54.6			67.9	153.1, 158.0, 160.5
					70.4	
					76.9	
5	227.8	59.2	83.9	19.2	66.5	124.4, 124.8, 126.1, 127.2, 138.0,
					71.7	140.7, 150.4, 151.8, 153.5, 157.9
6	220.6	51.7	75.6	18.0	67.4	124.6, 124.9, 126.8, 127.5, 138.0,
					72.6	141.1, 150.6, 151.9, 153.7, 158.4

[a] 67.8 MHz, $(CD_3)CO$, δ ppm at 293 K. [b] Free bpma: 60.0, 121.9, 122.0, 136.4, 149.2, 159.8; free tpma: 60.1, 121.9, 122.9, 136.4, 149.0, 159.2.

Table 4

Interatomic distances (Å) and angles (deg) with standard deviations in parentheses for $[W(CO)_2(\eta^3\text{-}C_3H_5)(bpma)]PF_6$

W1–N1	2.21(1)	W2–N4	2.26(1)
W1–N2	2.26(1)	W2–N5	2.25(1)
W1–N3	2.26(1)	W2–N6	2.23(1)
W1–C1	1.96(2)	W2–C18	1.95(2)
W1–C2	1.89(2)	W2–C19	1.91(2)
W1–C3	2.33(2)	W2–C20	2.35(2)
W1–C4	2.35(2)	W2–C21	2.22(2)
W1–C5	2.23(2)	W2–C22	2.35(2)
C1–O1	1.17(2)	C19–O3	1.20(2)
C2–O2	1.24(2)	C18–O4	1.16(2)
C3–C5	1.49(2)	C20–C21	1.45(2)
C4–C5	1.41(3)	C21–C22	1.45(2)
N1–W1–N2	74.7(4)	N4–W2–N5	75.0(4)
N1–W1–N3	76.6(4)	N4–W2–N6	76.4(4)
N2–W1–N3	74.7(4)	N5–W2–N6	73.7(4)
C1–W1–C2	83.4(7)	C18–W2–C19	81.8(7)
C3–W1–C4	62.4(6)	C20–W2–C21	36.7(5)
C3–W1–C5	38.0(5)	C20–W2–C22	62.3(6)
C4–W1–C5	35.8(6)	C21–W2–C22	36.8(6)
W1–C1–O1	178(1)	W2–C18–O4	179(1)
W1–C2–O2	179(1)	W2–C19–O3	177(1)
C3–C5–C4	114(1)	C20–C21–C22	114(1)

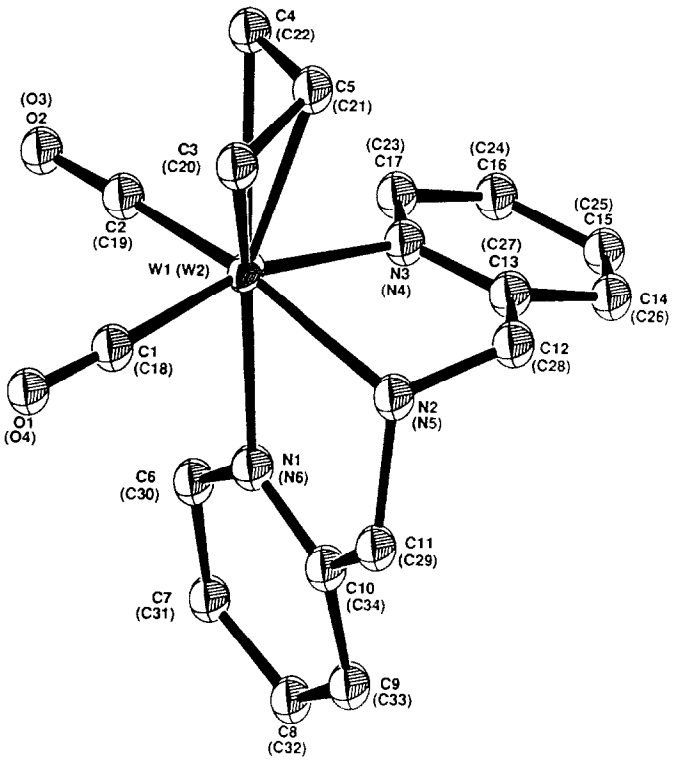

Fig. 1. ORTEP plot (33% ellipsoids) of $[W(CO)_2(\eta^3\text{-}C_3H_5)(bpma)]PF_6$ (**1a**) with atom-labelling scheme used. Labels for the second molecule in the unit cell are given in parentheses.

pseudooctahedral arrangement of ligands in which the two carbonyls and the η^3-allyl ligand are mutually cis to each other, with the terminal carbon atoms of the allyl group oriented over the carbonyls. Such an arrangement has been shown to be energetically favourable [5], and is that found experimentally [4,6–10] in all but one complex [11] of this type. Of the two possible orientations of the tridentate ligand on the opposite triangular face of the pseudooctahedron, the bpma ligand adopts the unsymmetrical bonding mode, so giving rise to a chiral centre at tungsten and enantiomers of type Ia and Ib. The three W–N separations at 2.21(1), 2.26(1) and 2.26(1) Å for W(1)–N(1), W(1)–N(2) and W(1)–N(3), respectively (and at 2.26(1), 2.25(1) and 2.23(1) Å for the second molecule in the unit cell) are noticeably different, with the pyridine ring sited *trans* to the allyl group most strongly bonded to the metal centre. As the ring nitrogens are expected to be better σ-donors than the exocyclic nitrogen, the dissimilarities in the W–C and C–O carbonyl distances (W(1)–C(2) 1.89(2) and C(2)–O(2) 1.24(2); W(1)–C(1) 1.96(1) and C(1)–O(1) 1.17(2) Å) trans to these two types of donor are commensurate with this trend. Two 5-membered rings sharing W(1)–N(2) (W(2)–N(5) in the second molecule in the unit cell) as a common edge can be identified, each comprising the metal, two N atoms, a methylene C and one pyridyl ring carbon. Bond lengths and angles within these rings are very similar with an average N–W–N angle of 75(1)°. The pyridyl rings are approximately planar and the plane

Table 5

Structural parameters for the allyl ligand in complexes with an unsymmetric structure of type I

Complex	Separation	C_c-C_t (Å)	$\Delta(C_c-C_t)$	$C_t-C_c-C_t$	Reference
$[W(bpma)(CO)_2(\eta^3-C_3H_5)]PF_6$ (1) [a]	1.45 (2)	1.45 (2)	0.000 (4)	114 (1)	This work
	1.41 (3)	1.49 (2)	0.08 (5)	114 (1)	
$[Mo(bpam)(CO)_2(\eta^3-C_3H_5)]PF_6$ [a]	1.44 (1)	1.45 (1)	0.01 (2)	110.3 (5)	3
	1.41 (1)	1.56 (1)	0.15 (2)	123.2 (6)	
$Mo(H_2B(Me_2pz)_2)(CO)_2(\eta^3-C_3H_5)$	1.35 (1)	1.42 (1)	0.07 (2)	118.4 (4)	6
$Mo(acac)(py)(CO)_2(\eta^3-C_3H_5)$	1.37 (1)	1.40 (1)	0.03 (2)	115.1 (6)	7
$Mo(dppe)Cl(CO)_2(\eta^3-C_3H_5)$	1.40 (2)	1.40 (2)	0.00 (4)	116 (1)	8
$Mo(PhHC(Me_2pz)_2)Br(CO)_2(\eta^3-C_3H_5)$	1.39 (1)	1.39 (1)	0.00 (2)	118.6 (8)	9

[a] Two molecules in the unit cell. C_c and C_t refer to the central and terminal carbon atoms of the allyl ligand.

containing pyridyl ring N(1) is skewed at an angle of 72(1)° relative to the plane containing C(5)–W(1)–N(1), which bisects the angle C(1)–W(1)–C(2). Thus this complex has several structural features in common with those of $[Mo(CO)_2(\eta^3-C_3H_4Me)(MeGa(3,5\text{-}Me_2pz)_2OH)]$ (pz = pyrazolyl) [12] which exhibits similar 5-membered ring systems twisted to avoid strain about the congested metal centre. In view of the significant difference in structural parameters found for the allyl ligand in the two molecular forms contained within the unit cell of the molybdenum complex $[Mo(bpam)(CO)_2(\eta^3-C_3H_5)]PF_6$ [2], it is interesting to compare analogous parameters in this structurally similar tungsten complex. Relevant data are presented in Table 5 together with bond lengths and angles (Δ) exhibited by other $[Mo(L_2)(L')(CO)_2(\eta^3-C_3H_5)]$ compounds with an unsymmetrical structure of type I. From these data it appears that inequivalent donor ligands *trans* to the carbonyl ligands do not necessarily induce asymmetry in the η^3-bonding mode of the allyl ligand. This is in keeping with our preliminary results from an EHMO exploration of the geometry and bonding of η^3-allyl complexes of d^4–d^8 metal species, which indicates that the $\psi_1(\text{allyl}) \rightarrow d_z^2$ interaction predominates over other interactions in η^3-allyl complexes of d^4 ions [13], and as a consequence changes in σ-donation from ligands *cis* to the allyl group are not expected *a priori* to induce distortions within the allyl group. It is interesting to note that there are also examples reported in the literature of allyl complexes with symmetric structures of type II, which contain highly distorted allyl ligands [14], and we are currently probing their solid-state structures and solution behaviour in more detail in order to determine whether electronic or crystal packing effects are responsible for these observations.

Replacement of the tridentate ligand bpma by the potentially quadridentate ligand tpma in these $M(CO)_2(\eta^3-C_3H_5)$ containing species is sufficient to change the solid state structural type, and also alter the solution properties of these complexes. Thus in **3**, tpma is found to behave as a tridentate ligand, and the cation adopts a symmetrical form (structural type II) in the solid state (Fig. 2 and Table 6). In this arrangement, all three metal-ligated N-bond distances are the same within experimental error (average 2.28(1) Å) irrespective of the different basicities expected for these donors, and the allyl ligand is symmetrically bonded to molybdenum. Surprisingly, the two carbonyl ligands exhibit significantly different

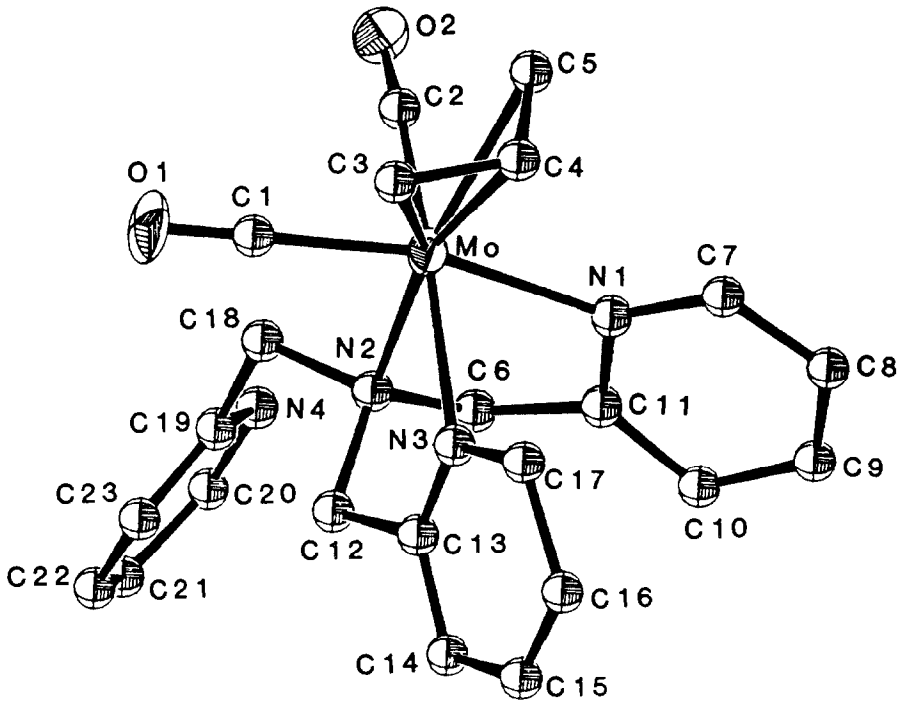

Fig. 2. ORTEP plot of $[Mo(CO)_2(\eta^3\text{-}C_3H_5)(tpma)]PF_6$ (**3**) with atom-labelling scheme used and 33% ellipsoids.

Mo–C (1.94(2) and 2.05(2) Å) and C–O (1.17(2) and 1.07(2) Å) separations, but there do not appear to be close contacts with other atoms which might account for this observation. The coordinated pyridyl rings are approximately planar, and show N(1)–Mo–N(3), N(2)–Mo–N(1) and N(2)–Mo–N(3) angles which are within 1° of those found in **1a**. The third and uncoordinated pyridyl ring is constrained to lie in a "folded back" position beneath the carbonyl ligands (Fig. 2). Our limited

Table 6

Interatomic distances (Å) and angles (deg) with standard deviations in parentheses for $[Mo(CO)_2(\eta^3\text{-}C_3H_5)(tpma)]PF_6$

Mo1–N1	2.28(1)	Mo1–N2	2.29(2)
Mo1–N3	2.29(1)	Mo1–C1	1.94(2)
Mo1–C2	2.05(2)	Mo1–C3	2.35(2)
Mo1–C4	2.22(2)	Mo1–C5	2.33(2)
C1–O1	1.17(2)	C2–O2	1.07(2)
C3–C4	1.42(2)	C4–C5	1.44(2)
N1–Mo1–N2	75.7(5)	N1–Mo1–N3	76.2(4)
N2–Mo1–N3	74.1(5)	C1–Mo1–C2	85.3(6)
C3–Mo1–C4	36.0(5)	C3–Mo1–C5	62.4(6)
C4–Mo1–C5	36.8(6)	Mo1–N2–C18	112(1)
Mo1–C1–O1	176(1)	Mo1–C2–O2	176(1)
C3–C4–C5	116(1)		

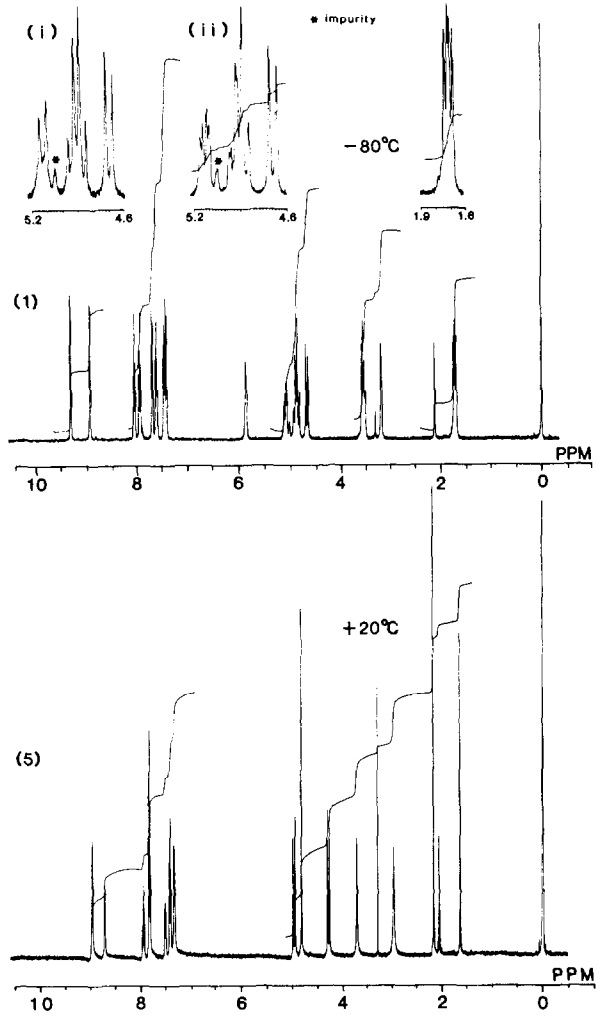

Fig. 3. Variable temperature ^{1}H NMR spectra of **1** and **5**, showing decoupled (i) and coupled (ii) spectra of the ligand methylene protons of **1** at low temperature.

attempts to induce the tpma ligand to behave as a quadridentate, which would necessitate either displacement of CO, or an $\eta^3 \rightarrow \eta^1$ conversion of the allyl ligand, have failed to date to produce evidence of the existence of either species as a stable entity.

NMR spectra of 1–6

Both ^{1}H and ^{13}C NMR spectra were obtained at ambient temperature, and limiting low-temperature and high-temperature proton NMR spectra were recorded for representative examples of these complexes. Data are summarized in Tables 2 and 3, and illustrated for **1** and **5** in Fig. 3 and for **4** in Fig. 4. Dissolution of either form of **1** generates solutions with the same NMR spectra, which at low temperature reveal the presence of only one major species (as an enantiomeric pair). For

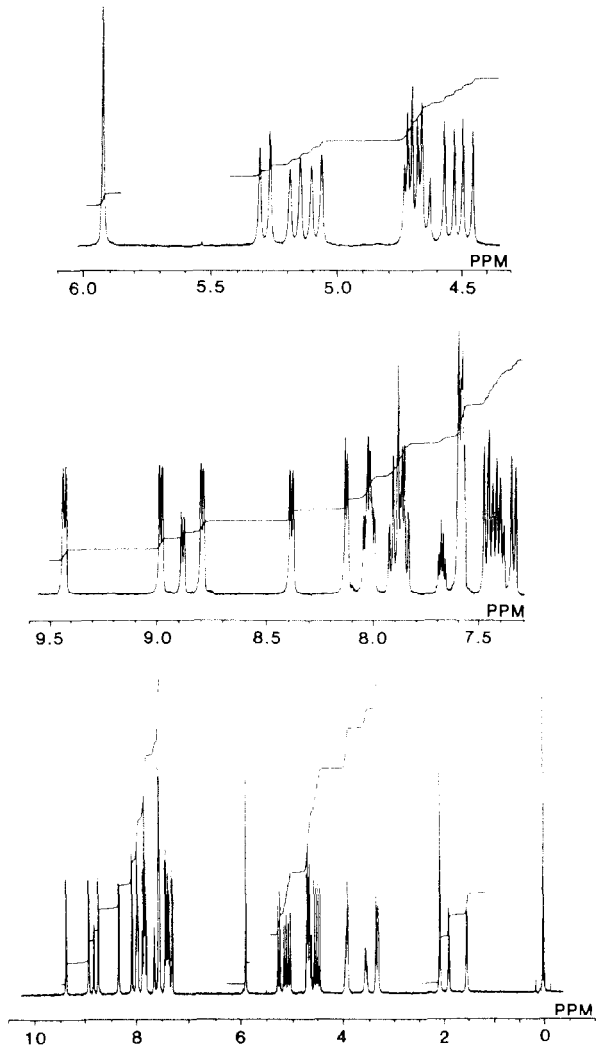

Fig. 4. Low temperature (−50°C) ^{1}H NMR spectrum of **4** with an expansion of ligand resonances.

this cation, two different chemical environments for the aromatic rings of the bpma ligand are apparent from the splitting of each of the three sets of aromatic proton signals into two components of equal intensities, and separate resonances are observed for each of the *syn*- and *anti*-allyl protons, in keeping with the structure found for the solid complex. The ligand methylene signals are observed at about 5 ppm as an AA′BB′ pattern (Fig. 3) in which NH coupling to only two of the four protons is observed in the limiting low temperature spectrum. Based on the solid state structure of **1a**, and a regular tetrahedral distribution of H atoms around C(11), C(12) and N(2) (Fig. 5), the dihedral angles H(111)–C(11)–N(2)–N(2)H and H(122)–C(12)–N(2)–(2)H are 31° and 25°, respectively, whereas the corresponding values for H(112)–C(11)–N(2)–N(2)H and H(121)–C(12)–N(2)–N(2)H are 90° and

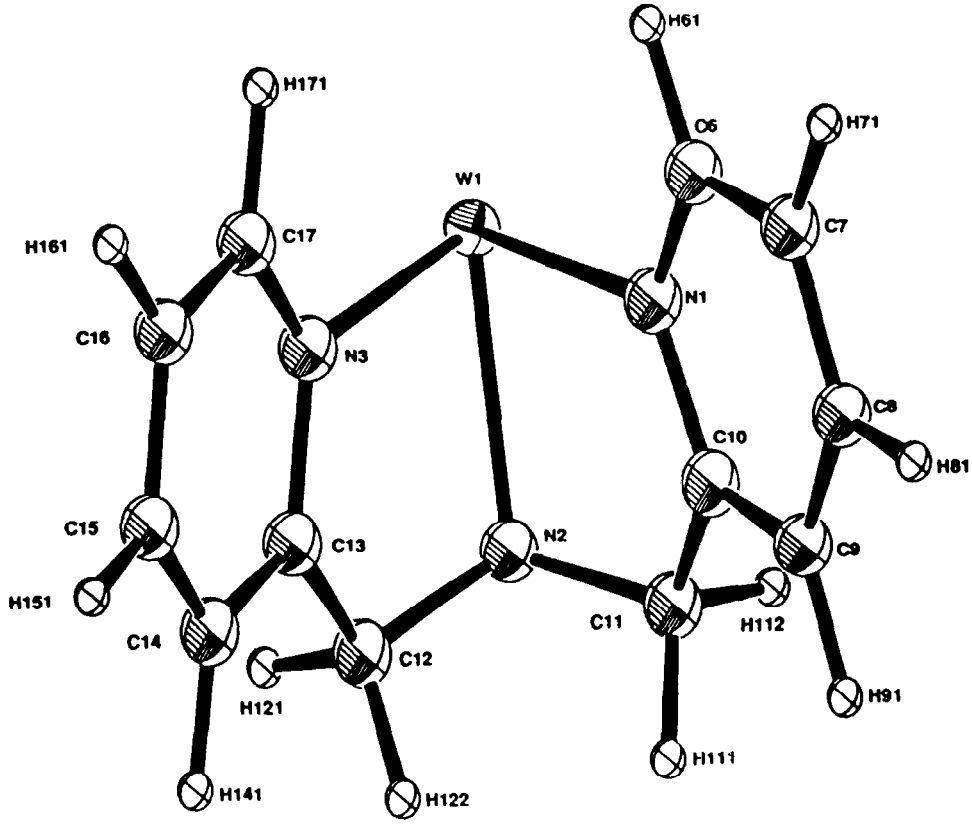

Fig. 5. ORTEP view of the bpma ligand in $[W(CO)_2(\eta^3\text{-}C_3H_5)(bpma)]PF_6$ (hydrogen atoms at idealized positions).

95°. *Vicinal* interproton coupling involving NH is only expected [15] to be significant for H(111) and H(122) therefore, in keeping with the experimental observations. Above room temperature the cation is dynamic, and the two sets of signals for H_{anti} and H_{syn} of the allyl ligand, and for the aromatic protons, coalesce. In addition the bpma methylene AA'BB' pattern simplifies, but NH coupling to half of the multiplet is retained. Complex **2** exhibits very similar spectral features, but reaches the limiting high temperature spectrum at lower temperatures than **1**. The room temperature $^{13}C\{^1H\}$ NMR data for both these complexes are exceedingly simple with single resonances observed for CO, C(terminal), and C(central) of the allyl ligand, and for C(methylene) of the tridentate ligand, respectively. These data are in accord with an unsymmetrical structure of type I at low temperature, with rapid interconversion between *S* and *R* conformations at ambient temperature by a process which preserves the inequivalence, with respect to the NH group, of two of the four methylene hydrogens of the tridentate ligand. A non-dissociative trigonal twist rearrangement is consistent with these observations. Such a process has been proposed for other $[Mo(CO)_2(\eta^3\text{-}C_3H_5)L_3]$ species [1,10,16] as well as for several neutral molybdenum-allyl complexes of the type $[Mo(CO)_2(\eta^3\text{-}C_3H_5)(L_2)X]$ (L_3 = neutral tridentate ligand, L_2 = anionic bidentate and X =

Table 7

Fractional atomic coordinates and thermal parameters (Å) for **1a**

Atom	x	y	z	U_{iso} or U_{eq} [a]
W1	0.05763(5)	0.05887(3)	0.19948(3)	0.0319(3) [a]
P1	0.0643(3)	0.3134(2)	0.0312(2)	0.040(2) [a]
F1	0.1502(8)	0.2986(4)	0.1108(5)	0.060(6) [a]
F2	−0.0167(7)	0.3435(5)	0.0874(5)	0.065(6) [a]
F3	0.1166(8)	0.3862(5)	0.0270(6)	0.070(7) [a]
F4	−0.0225(8)	0.3288(5)	−0.0474(5)	0.063(6) [a]
F5	0.1445(8)	0.2833(6)	−0.0248(6)	0.078(7) [a]
F6	0.0105(8)	0.2414(4)	0.0385(6)	0.071(7) [a]
W2	0.45453(5)	0.15468(3)	0.92240(3)	0.0351(3) [a]
P2	0.3332(4)	0.5669(2)	0.1723(3)	0.053(3) [a]
F7	0.2153(10)	0.5675(10)	0.1245(7)	0.143(13) [a]
F8	0.3802(10)	0.5623(8)	0.0903(6)	0.120(10) [a]
F9	0.3429(17)	0.6448(6)	0.1739(11)	0.175(16) [a]
F10	0.4504(10)	0.5647(9)	0.2213(8)	0.136(12) [a]
F11	0.2841(9)	0.5699(5)	0.2544(6)	0.076(7) [a]
F12	0.3257(15)	0.4880(7)	0.1744(10)	0.154(14) [a]
O1	−0.1450(11)	0.0874(6)	0.0679(8)	0.080(4)
O2	0.1816(10)	0.0836(6)	0.0536(7)	0.073(3)
N1	0.0368(9)	−0.0503(5)	0.1728(6)	0.036(3)
N2	−0.0277(8)	0.0170(5)	0.2988(6)	0.032(3)
N3	0.1891(9)	0.0104(5)	0.2891(6)	0.034(3)
C1	−0.0703(12)	0.0770(7)	0.1183(9)	0.048(4)
C2	0.1329(13)	0.0744(8)	0.1118(9)	0.055(4)
C3	−0.0244(13)	0.1597(8)	0.2292(9)	0.053(4)
C4	0.1682(13)	0.1550(9)	0.2234(10)	0.061(4)
C5	0.0875(13)	0.1523(8)	0.2738(9)	0.055(4)
C6	0.0948(12)	−0.0813(7)	0.1193(9)	0.049(4)
C7	0.0907(12)	−0.1510(8)	0.1104(9)	0.053(4)
C8	0.0353(13)	−0.1877(8)	0.1588(9)	0.056(4)
C9	−0.0216(11)	−0.1571(7)	0.2143(8)	0.043(3)
C10	−0.0206(10)	−0.0876(6)	0.2186(7)	0.032(3)
C11	−0.0839(11)	−0.0475(7)	0.2702(8)	0.043(3)
C12	0.0486(11)	0.0095(7)	0.3747(8)	0.038(3)
C13	0.1573(11)	−0.0109(7)	0.3592(8)	0.038(3)
C14	0.2318(13)	−0.0480(8)	0.4146(9)	0.054(4)
C15	0.3292(13)	−0.0648(8)	0.3960(9)	0.056(4)
C16	0.3595(14)	−0.0434(8)	0.3264(10)	0.060(4)
C17	0.2868(12)	−0.0047(7)	0.2719(9)	0.048(4)
O3	0.5370(10)	0.1863(6)	0.7603(8)	0.080(4)
O4	0.5815(10)	0.0219(6)	0.9025(7)	0.076(3)
N4	0.4018(9)	0.2587(5)	0.9556(6)	0.037(3)
N5	0.4265(9)	0.1457(6)	1.0510(6)	0.042(3)
N6	0.6017(9)	0.1968(5)	0.9984(6)	0.037(3)
C18	0.5339(13)	0.0714(8)	0.9107(9)	0.055(4)
C19	0.5028(13)	0.1752(8)	0.8223(9)	0.052(4)
C20	0.3327(13)	0.0633(8)	0.9009(9)	0.053(4)
C21	0.2805(12)	0.1285(8)	0.8867(9)	0.051(4)
C22	0.3076(14)	0.1640(9)	0.8167(10)	0.067(5)
C23	0.4109(12)	0.3145(7)	0.9074(9)	0.049(4)
C24	0.3969(13)	0.3785(8)	0.9355(9)	0.056(4)
C25	0.3815(13)	0.3867(9)	1.0133(10)	0.061(4)
C26	0.3749(13)	0.3323(8)	1.0620(10)	0.058(4)
C27	0.3854(11)	0.2675(7)	1.0301(8)	0.038(3)

Table 7 (continued)

Atom	x	y	z	U_{iso} or U_{eq} [a]
C28	0.3657(12)	0.2044(7)	1.0780(9)	0.046(4)
C29	0.5326(12)	0.1381(7)	1.1057(9)	0.048(4)
C30	0.6682(11)	0.2399(7)	0.9676(9)	0.044(4)
C31	0.7485(13)	0.2729(8)	1.0187(10)	0.059(4)
C32	0.7580(12)	0.2627(8)	1.1018(9)	0.051(4)
C33	0.6915(13)	0.2184(8)	1.1312(9)	0.052(4)
C34	0.6129(11)	0.1865(7)	1.0768(8)	0.039(3)

[a] $U_{eq} = \sum_{i=1,3} u_{ii}$.

neutral monodentate) [7,8]. For these latter examples, the interconversion of enantiomers need not involve the intermediacy of a symmetrical species. Indeed, it has been shown that Mo(acac)(py)$(CO)_2(\eta^3\text{-}C_3H_5)$ (acac = acetylacetonate anion, py = pyridine) exists in $CHCl_3$ as a mixture of isomers of type I and II, with the former being dynamic at temperatures well below which interconversion between I and II occurs [7]. However, for unsymmetrical complexes containing a tridentate ligand such as bpma, a trigonal twist rearrangement must proceed via a symmetrical species of type II, but whether or not both geometric isomers I and II coexist as stable species appears from the limited information available to be highly dependent upon a combination of both steric and electronic factors.

NMR data for complexes **3–6**, all of which contain the potentially quadridentate ligand tpma, exhibit different features from those described above. ^{1}H NMR measurements at low temperatures indicate that complexes **3** and **4** are present in acetone solutions as a mixture of two isomers in the approximate ratio 2:1. Both contain an uncoordinated pyridine ring, with the minor isomer having the symmetric structure found in the solid state for **3**, and the major isomer having an unsymmetrical structure of type I. Diagnostic features are most clearly seen in the proton signals for the *ortho*-protons in the pyridine rings of tpma. Thus for **4** at −50°C (Fig. 4), signals at 9.42 and 8.97 ppm of equal intensities are assigned to the coordinated pyridine rings of the cation of structural type I. The *ortho*-proton of the uncoordinated pyridine ring resonates at 8.80 ppm, in a similar position to the analogous resonances of the free ligand. Signals at 8.37 and 8.87 ppm in the ratio 2:1 are assigned to coordinated and free pyridine rings in the symmetric isomer (type II). The methylene signals of the tpma ligand in the two isomers can also be assigned. The symmetric isomer exhibits doublets at 4.70 and 5.30 ppm for protons on C(6) and C(12), and a sharp singlet at 5.95 ppm for the methylene protons of the uncoordinated $-CH_2$py arm of the ligand. The low symmetry of the second isomer gives rise to four doublets for the C(6) and C(12) protons, and an AB quartet for the methylene protons of the free $-CH_2$py group. Molecular models show that protons on C(18) suffer steric constraint in structural type I because of the proximity of the terminal methylene group of the allyl ligand. Two sets of allyl protons are also discernible, and homonuclear ^{1}H-^{1}H COSY measurements permitted the connectivities noted in Table 2. As the temperature is raised, peak broadening and then coalescence of the two sets of signals occurs, and finally a simplified spectrum is obtained in which there is no longer evidence of either two isomers or a unique, uncoordinated pyridine ring in the cation. The spectrum of

complex **3** shows a similar variation with temperature, but overlapping signals prevented definitive assignments. We were not able in either case to determine whether interconversion between structural types I and II was independent of, or concomitant with, donor centre exchange of the tpma ligand. The complexity of the room temperature ^{13}C NMR data recorded on **3** and **4** is also indicative of more than one isomer for each complex, but assignments have not been attempted in view of the incomplete resolution of all expected signals. Neither of the 2-MeC_3H_4 containing analogues, **5** or **6**, exhibit dynamic properties over the temperature range −90 to +50°C as evidenced by their ^1H NMR spectra. Their spectral properties are consistent with the existence in solution of a single, symmetric isomer of type II, in which tpma acts as a tridentate. ^1H and ^{13}C resonances of the methylene group of the uncoordinated $-CH_2py$ arm of the ligand appear as singlets at approx. 4.8 ppm and approx. 67 ppm in their respective spectra, compared with AB quartets for the chemically equivalent methylene protons of the ligated $-CH_2py$ arms (Fig. 3), and ^{13}C resonances at approx. 72 ppm.

Conclusions

In earlier studies, we showed that replacement of H by Me in the 2-position of the allyl ligand causes significant changes in the dynamic behaviour and solution structure of some $MoX(CO)_2(\eta^3\text{-allyl})(L_2)$ complexes [4,17]. For cationic species $[W(CO)_2(\eta\text{-allyl})(L_3)]^+$ containing the neutral tridentate ligand bpma, no major changes of this type are observed. However, replacement of the tridentate secondary amine bpma by the potentially quadridentate tertiary amine tpma in the metal coordination sphere of $M(CO)_2(\eta^3\text{-}C_3H_5)$ containing cations (M = Mo, W), does not result in a change in the donor set, but does result in significant changes in the type of solid-state structure adopted by the cation. In addition, these ions exist at low temperatures in solution in two isomeric forms in which tpma acts as a tridentate, but at elevated temperatures these isomers interconvert, and fast exchange occurs between the coordinated and uncoordinated pyridyl rings. By contrast $[M(CO)_2(\eta^3\text{-}2\text{-}MeC_3H_4)(L_4)]^+$ exists as a single isomer in solution over the temperature range −90 to +50°C, with tpma coordinated via the exocyclic N atom and two of the three pyridyl rings, and no evidence of an L_4 rearrangement process as in **3** and **4**.

These systems reveal the very precise steric control available to determine the stereochemistry and dynamic behaviour of $M(CO)_2(\eta^3\text{-allyl})$ containing moieties. In view of the importance of such compounds as intermediates in catalytic allylic alkylation reactions [18], and the relationship suggested between the stereochemistry of the intermediate and the identity of the organic product [19], these compound are of interest as models for further studies.

Experimental section

Starting materials

The complexes of the type $MCl(CO)_2(\eta^3\text{-}C_3H_4R)(NCMe)_2$ (M = Mo, W; R = H or Me) were prepared using literature methods [17,20]. The ligand bpma was prepared by the reaction of 2-chloromethylpyridine with 2-aminomethylpyridine

[21]. Bpma was also initially used to synthesise tpma, using the procedure described by Nelson *et al.* [22]. In the later stages of this study, a direct procedure for the preparation of tpma was developed as noted below. Acetonitrile was dried and distilled prior to use. Reactions were carried out in a nitrogen atmosphere.

Synthesis of tris(2-aminomethyl)pyridine (tpma)

A solution of 2-chloromethylpyridine hydrochloride (35.5 g, 0.22 mol) in water (50 cm^3) was made alkaline with an aqueous slurry of K_2CO_3 until effervesence ceased and a red oil formed. This mixture was extracted with diethyl ether (4×50 cm^3), dried over $CaSO_4$, and after filtration, the solvent was removed *in vacuo*. The residue was dissolved in ethanol (150 cm^3) and cooled in ice. To this was added dropwise with care 2-aminomethylpyridine (11.9 g, 0.11 mol) and the mixture refluxed for 18 h. Solvent was removed *in vacuo* from the cooled solution, and the oily residue dissolved in water (100 cm^3), made alkaline with K_2CO_3 and continuously extracted with dichloromethane (5×50 cm^3). The dark red liquid was dried over $CaSO_4$, filtered and the solvent removed *in vacuo*. On vacuum distillation, a white vapour was produced, and this resulted in the formation of a white crystalline material in the condenser and still-head. Recrystallization of this solid from benzene yielded the product as long, white needles in 60% yield, m.p. 84.5–87.0°C (85.5–86.5°C lit. [23]).

Synthesis of $[W(CO)_2(\eta^3\text{-}C_3H_4R)L_3]PF_6$ *and* $[M(CO)_2(\eta^3\text{-}C_3H_4R)L_4]PF_6$ *(M = Mo, W; R = H, Me;* L_3 *= bpma,* L_4 *= tpma)*

A solution of $MCl(CO)_2(\eta^3\text{-}C_3H_4R)(NCMe)_2$ (5.0 mmol) in acetonitrile (25 cm^3) was heated under reflux for 1 h with bpma or tpma (5.0 mmol). The mixture was then cooled, solvent removed *in vacuo* and the residue dissolved in water (100 cm^3), and treated dropwise with a solution of NH_4PF_6 (1.0 g) dissolved in water (10 cm^3). The crude product which precipitated as an orange solid, was removed by filtration after 1 h, washed with water, dried, and recrystallized from aqueous acetone (complexes **1** and **2**) or aqueous methanol (complexes **3**–**6**).

No further reaction occurred on heating or irradiating a solution of **3** under reflux for 12 h in either acetone or benzonitrile.

Preparation of crystals for X-ray analysis

Samples of **1** and **3** were recrystallized from aqueous acetone (1 : 1). Crystals of approximate dimensions $0.15 \times 0.2 \times 0.2$ mm and $0.2 \times 0.2 \times 0.3$ mm, respectively, were used for data collection. Data were measured at room temperature on a Hilger and Watts Y290 four-circle diffractometer in the range $2 \leq \theta \leq 22°$. Data were corrected for Lorentz and polarization effects but not for absorption. The structures were solved by Patterson methods and refined using the SHELX suite of programs [24,25].

Crystal data for ***1a****.* $C_{17}H_{18}O_2N_3PF_6W$, $M = 625.15$, monoclinic, $a = 12.489(5)$, $b = 19.780(4)$, $c = 16.698(4)$ Å, $\beta = 98.98(2)°$, $U = 4072.2$ Å^3, space group $P2_1/c$, $Z = 8$, $D_c = 2.04$ g cm^{-3}, μ(Mo-K_α) = 56.90 cm^{-1}, $F(000) = 2400$; 5425 reflections were collected of which 3592 were unique with $I \geq 3\sigma(I)$. The asymmetric unit consisted of two molecules of the salt which were of the same gross geometrical structure. In the final least squares cycles, the tungsten, fluorine and phosphorus atoms were allowed to vibrate anisotropically, and all other atoms were treated

isotropically. Hydrogen atoms were included at calculated positions. Both cations and anions were refined in blocks during the final stages of convergence. Final residuals after 24 cycles of least squares were $R = 0.0426$ and $R_w = 0.0426$. Maximum final shift/e.s.d. was 0.007, the average being 0.003. The maximum and minimum residual densities were 0.83 and -0.80 e $Å^{-3}$, respectively. Final fractional atomic coordinates and isotropic thermal parameters are given in Table 7. Tables of bond distances and angles, anisotropic temperature factors and hydrogen atom positions are available as supplementary data (Tables S1, S2, S3 and S4, respectively). The asymmetric unit is shown in Fig. 1, along with the labelling scheme used.

Table 8

Fractional atomic coordinates and thermal parameters (Å) for **3**

Atom	x	y	z	U_{iso} or U_{eq} [a]
Mo1	0.63136(6)	0.58151(18)	0.63625(5)	0.0465(9) [a]
O1	0.6935(6)	0.6385(18)	0.7551(4)	0.085(10) [a]
O2	0.5095(5)	0.6432(16)	0.6671(4)	0.074(9) [a]
P1	0.1207(3)	0.1296(7)	0.4231(2)	0.082(5) [a]
F1	0.1589(5)	0.2525(15)	0.4634(4)	0.100(10) [a]
F2	0.0834(8)	−0.0014(19)	0.3870(5)	0.133(13) [a]
F3	0.0809(8)	0.2628(19)	0.3870(5)	0.139(14) [a]
F4	0.1528(6)	−0.0012(18)	0.4615(5)	0.121(12) [a]
F5	0.0708(6)	0.1329(20)	0.4553(5)	0.135(14) [a]
F6	0.1714(8)	0.1328(24)	0.3942(6)	0.193(18) [a]
N1	0.5876(5)	0.4654(17)	0.5581(5)	0.053(3)
N2	0.6256(5)	0.3375(17)	0.6586(5)	0.050(3)
N3	0.7133(5)	0.4658(16)	0.6176(4)	0.046(3)
N4	0.5402(8)	0.0923(27)	0.7132(7)	0.107(6)
C1	0.6714(7)	0.6206(22)	0.7100(7)	0.060(5)
C2	0.5500(8)	0.6235(21)	0.6546(6)	0.055(4)
C3	0.6914(7)	0.7998(23)	0.6478(6)	0.061(5)
C4	0.6475(7)	0.7905(22)	0.5974(6)	0.056(4)
C5	0.5831(8)	0.7980(25)	0.5968(7)	0.073(5)
C6	0.5799(7)	0.2539(23)	0.6156(6)	0.059(5)
C7	0.5812(6)	0.5234(22)	0.5105(5)	0.051(4)
C8	0.5719(6)	0.4374(24)	0.4660(6)	0.060(4)
C9	0.5684(6)	0.2899(22)	0.4698(6)	0.052(4)
C10	0.5732(6)	0.2208(22)	0.5179(5)	0.054(4)
C11	0.5827(7)	0.3157(22)	0.5615(6)	0.053(4)
C12	0.6890(7)	0.2753(25)	0.6706(7)	0.072(5)
C13	0.7216(7)	0.3377(23)	0.6321(5)	0.049(4)
C14	0.7581(9)	0.2406(31)	0.6142(8)	0.096(7)
C15	0.7923(11)	0.3011(37)	0.5800(9)	0.115(8)
C16	0.7857(9)	0.4367(35)	0.5672(9)	0.101(7)
C17	0.7446(7)	0.5225(24)	0.5865(6)	0.064(5)
C18	0.6013(8)	0.3204(24)	0.7076(6)	0.067(5)
C19	0.5985(7)	0.1659(24)	0.7267(6)	0.063(5)
C20	0.5383(9)	−0.0568(27)	0.7338(7)	0.079(6)
C21	0.5915(8)	−0.1116(27)	0.7668(7)	0.079(6)
C22	0.6450(9)	−0.0291(28)	0.7761(7)	0.085(6)
C23	0.6499(7)	0.1026(23)	0.7573(6)	0.055(4)

[a] $U_{eq} = \sum_{i=1,3} u_{ii}$.

Crystal data for 3. $C_{23}H_{23}O_2N_4PF_6Mo$, $M = 628.3$, monoclinic, $a = 22.442(6)$, $b = 9.004(4)$, $c = 26.463(6)$ Å, $\beta = 106.4(2)°$, $U = 5129.4$ Å^3, space group $I2/a$ (non-standard $C2/c$), $Z = 8$, $D_c = 1.63$ g cm^{-3}, μ(Mo-K_α) = 5.62 cm^{-1}, $F(000) = 2472$. 3560 reflections were collected of which 1828 were unique with $I \geq 3\sigma(I)$. In the final least squares cycles, the molybdenum and oxygen atoms were allowed to vibrate anisotropically, and all other atoms were treated isotropically. Hydrogen atoms were included at calculated positions. Final residuals after 14 cycles of least squares were $R = 0.0883$ and $R_w = 0.0894$. Maximum final shift/e.s.d. was 0.014, the average being 0.004. The maximum and minimum residual densities were 0.33 and -0.51 e Å^{-3}, respectively. Final fractional atomic coordinates and isotropic thermal parameters are given in Table 8. Tables of bond distances and angles, anisotropic temperature factors and hydrogen atom positions are available as supplementary data (Tables S5, S6, S7 and S8). The asymmetric unit is shown in Fig. 2, along with the labelling scheme used.

References

1 B.J. Brisdon, M. Cartwright and A.G.W. Hodson, J. Organomet. Chem., 277 (1984) 85.
2 K.-B. Shiu, K.-S. Lion, C.P. Cheng, B.-R. Fang, Y. Wang, G.-H. Lee and W.J. Vong, Organometallics, 8 (1989) 1219.
3 K.-B. Shiu, C.-J. Chang, Y. Wang and M.-C. Chen, J. Organomet. Chem., 406 (1991) 363.
4 B.J. Brisdon and A. Day, J. Organomet. Chem., 221 (1981) 279; M.G.B. Drew, B.J. Brisdon and A. Day, J. Chem. Soc., Dalton Trans., (1981) 1310.
5 M.D. Curtis and O. Eisenstein, Organometallics, 3 (1984) 887.
6 N.W. Murrall and A.J. Welch, J. Organomet. Chem., 301 (1986) 109.
7 B.J. Brisdon and A.A. Woolf, J. Chem. Soc., Dalton Trans., (1978) 291.
8 J.W. Faller, D.A. Haitko, R.D. Adams and D.F. Chodosh, J. Am. Chem. Soc., 101 (1979) 865.
9 K.-B. Shiu, C.-J. Chang, S.-L. Wang and F.-L. Liao, J. Organomet. Chem., 407 (1991) 225.
10 V.S. Joshi, V.K. Kale, K.M. Sathe, A. Sarkar, S.S. Tavale and C.G. Suresh, Organometallics, 10 (1991) 2898.
11 B.J. Brisdon, D.A. Edwards, K.E. Paddick and M.G.B. Drew, J. Chem. Soc., Dalton Trans., (1980) 2129.
12 K.R. Breakall, S.J. Rettig, A. Storr and J. Trotter, Can. J. Chem., 57 (1979) 139.
13 B.J. Brisdon, R.J. Deeth and A. Moore, unpublished observations.
14 R.H. Fenn and A.J. Graham, J. Organomet. Chem., 37 (1972) 137; 17 (1969) 405.
15 H. Kessler and W. Bernel, Methods Stereochem. Anal., 6 (1986) 179, and refs. therein.
16 S. Trofimenko, J. Am. Chem. Soc., 91 (1969) 3183; Acc. Chem. Res., 14 (1971) 17.
17 B.J. Brisdon and M. Cartwright, J. Organomet. Chem., 164 (1979) 83.
18 B.M. Trost and M. Lautens, J. Am. Chem. Soc., 109 (1987) 1469.
19 B.M. Trost and M. Lautens, J. Am. Chem. Soc., 104 (1982) 5543.
20 B.J. Brisdon, M. Cartwright, D.A. Edwards and K.E. Paddick, Inorg. Chim. Acta, 40 (1980) 191.
21 J.K. Romary, J.D. Barger and J.E. Bunds, Inorg. Chem., 7 (1968) 1142.
22 M.M. da Mota, J. Rodgers and S.M. Nelson, J. Chem. Soc., (A), (1969) 2036.
23 G. Anderegg and F. Wenk, Helv. Chim. Acta, 50 (1967) 2330.
24 G.M. Sheldrick, SHELX86, A Computer Program for Crystal Structure Determination, University of Göttingen, 1986.
25 G.M. Sheldrick, SHELX76, A Computer Program for Crystal Structure Determination, University of Cambridge, 1976.